Animal Reproduction Science 235 (2021) 106882

Contents lists available at ScienceDirect

Animal Reproduction Science

journal homepage: www.elsevier.com/locate/anireprosci

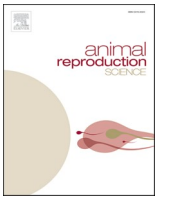

Proteomic fertility markers in ram sperm

Mustafa Hitit [a], Mehmet Özbek [b], Serife Ayaz-Guner [c], Huseyin Guner [c], Merve Oztug [d], Mustafa Bodu [e], Mesut Kirbas [f], Bulent Bulbul [g], Mustafa Numan Bucak [e], Mehmet Bozkurt Ataman [e], Erdoğan Memili [h,i,*], Abdullah Kaya [e,**]

[a] Department of Genetics, Faculty of Veterinary Medicine, Kastamonu University, Kastamonu, Turkey
[b] Department of Histology and Embryology, Faculty of Veterinary Medicine, Mehmet Akif Ersoy University, Burdur, Turkey
[c] Department of Molecular Biology and Genetics, Faculty of Life and Natural Science, Abdullah Gül University, Kayseri, Turkey
[d] National Metrology Institute, TUBITAK UME, Kocaeli, Turkey
[e] Department of Reproduction and Artificial Insemination, Faculty of Veterinary Medicine, Selcuk University, Konya, Turkey
[f] Bahri Dagdas International Agricultural Research Institute, Konya, Turkey
[g] Department of Reproduction and Artificial Insemination, Faculty of Veterinary Medicine, Dokuz Eylul University, Izmir, Turkey
[h] Department of Animal and Dairy Sciences, Mississippi State University, Starkville, MS, United States
[i] Cooperative Agricultural Research Center, College of Agriculture and Human Sciences, Prairie View A&M University, Prairie View, TX, United States

ARTICLE INFO

Keywords:
Ram
Sperm
Fertility
Proteomics

ABSTRACT

Precise estimation of ram fertility is important for sheep farming to sustain reproduction efficiency and profitability of production. There, however, is no conventional method to accurately predict ram fertility. The objective of this study, therefore, was to ascertain proteomic profiles of ram sperm having contrasting fertility phenotypes. Mature rams ($n = 66$) having greater pregnancy rates than average (89.4 ± 7.2%) were assigned into relatively-greater fertility (GF; $n = 31$; 94.5 ± 2.8%) whereas those with less-than-average pregnancy rates were assigned into a lesser-fertility (LF; $n = 25$; 83.1 ± 5.73%; $P = 0.028$) group. Sperm samples from the outlier greatest- and least-fertility rams ($n = 6$, pregnancy rate; 98.4 ± 1.8% and 76.1 ± 3.9%) were used for proteomics assessments utilizing Label-free LC-MS/MS. A total of 997 proteins were identified, and among these, 840 were shared by both groups, and 57 and 93 were unique to GF and LF, respectively. Furthermore, 190 differentially abundant proteins were identified; the abundance of 124 was larger in GF while 66 was larger in LF rams. The GF ram sperm had 79 GO/pathway terms in ten major biological networks while there were 47 GO/pathway terms in six biological networks in sperm of LF rams. Accordingly, differential abundances of sperm proteins between sperm of GF and LF rams were indicative of functional implications of sperm proteome on male fertility. The results of this study emphasize there are potential protein markers for evaluation of semen quality and estimation of ram sperm fertilizing capacity.

* Corresponding author at: Department of Animal and Dairy Sciences, Mississippi State University, Starkville, MS, United States.
** Corresponding author.
E-mail addresses: em149@ads.msstate.edu (E. Memili), akaya@selcuk.edu.tr (A. Kaya).

https://doi.org/10.1016/j.anireprosci.2021.106882
Received 13 May 2021; Received in revised form 22 October 2021; Accepted 23 October 2021
Available online 30 October 2021

1. Introduction

Male fertility, defined as the capacity of viable sperm to fertilize and activate the egg, and further support early embryonic development, is important in sheep production enterprises. As an economically relevant trait for sheep enterprises, ram fertility is a primary factor affecting flock performance of which the ram accounts for 50% (MacLaren, 1988; Pardos et al., 2008). Accordingly, proper management of rams before and during breeding seasons is important for reproductive efficiency, sustainability, and profitability of sheep production because ram fertility is markedly affected by environmental factors. The evaluation of the reproductive ability of rams using current methods, however, is ineffective, costly, and labor-intensive. There, therefore, is no conventional method to accurately predict ram fertility.

Precise estimation of ram fertility is necessary for the breeding industry to diminish male factor infertility associated with conception problems, and for farmers to reduce the production costs. Of these, sperm non-compensable factors are more likely to be related to a number of intrinsic determinants including damage or abnormalities in DNA, state of chromatin (Rathke et al., 2014), protamine protein markers and RNA molecules such as small noncoding RNAs (Capra et al., 2017; Dogan et al., 2015) that are associated with male fertility. In non-compensable fertility, molecular defects in sperm are not detectable using conventional methods. Results from recent studies have indicated there are underlying factors associated with male fertility using high-throughput "omics" research elucidating distinct transcriptomic, metabolomics, genomic and proteomic biomarkers (Hitit et al., 2020; Menezes et al., 2019, 2020; Özbek et al., 2021).

The striking evidence stemming from the use of innovative methods highlights the importance of proteomic methods because sperm remain transcriptionally "silent" beyond spermatogenesis (Pixton et al., 2004). Results from studies focused on quantitative proteomics of sperm indicated protein abundances are related to the quality of sperm, fertility, capacitation, and acrosome reaction (Netherton et al., 2018; Panner Selvam et al., 2019). The proteomic profiling of sperm as well as seminal plasma have highlighted the importance of protein markers associated with fertility and sperm freezability phenotypes (Dogan et al., 2015; Gomes et al., 2020; Muhammad Aslam et al., 2019). Also, in a previous report, the proteomes of sperm and seminal plasma (Pini et al., 2016), and proteomic profiles of ram sperm were postulated to be associated with sperm motility fertility markers (Zhu et al., 2020a). The objective of the present study, therefore, was to ascertain proteomic profiles of ram sperm where there were contrasting fertility phenotypes.

2. Materials and methods

2.1. Determination of ram fertility and experimental design

The fertility phenotypes of mature rams were provided by the Institute of Bahri-Dağdaş International Agricultural Research of the Republic of Turkey's Ministry of Agriculture and Forestry. Fertility of mature rams ($n = 66$) at least 4 years old was calculated based on pregnancy rates resulting from natural mating during the 2017, 2018, and 2019 breeding seasons.

The estrous detection of the ewes was performed by using "teaser" rams that were not allowed to mate by covering the prepuce area. The "teaser" rams were placed in a paddock with ewes for about 30 min early in the morning. The ewes that were seeking, standing for "teasing", and permitting mount attempts of the "teaser" rams were considered in estrus. Ewes expressing estrus were selected and moved into a pen where a randomly selected single ram was allowed for natural mating. During the entire breeding

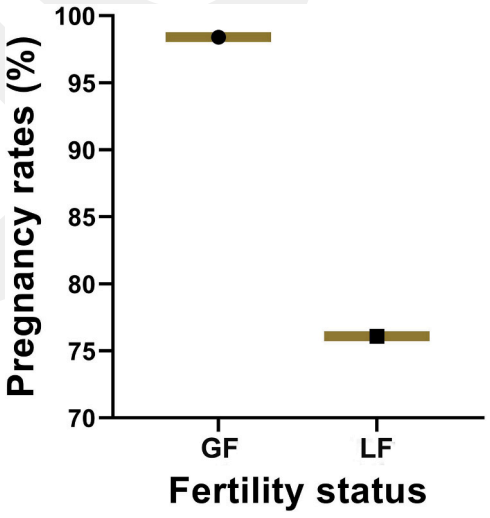

Fig. 1. Pregnancy rates of ewes mating with rams from the GF and LF groups for which sperm were evaluated by conducting proteomics analysis; Pregnancy rates were ranked with the least to greatest; Pregnancy rates (%), fertility status; relatively-greater (n = 6) and relatively-lesser (n = 6).

season, estrous detection was continued, and ewes were allowed to mate with a randomly selected ram. The ewes that did not return to estrus within 35 days after mating were considered to be pregnant. Furthermore, the numbers of pregnant and non-pregnant ewes were confirmed for each ram by matching the mating and lambing dates based on the average duration of ewe gestational periods.

Fertility scores of the rams were ranked based on conception rates. The average pregnancy rate was 89.4 ± 7.2% ($n = 66$) and, the rams having greater pregnancy rates than the average were assigned into a relatively-greater fertility (GF) group ($n = 31$; 94.5 ± 2.8%) whereas rams with a lesser than average value were assigned to a relatively-lesser fertility (LF) group ($n = 25$; 83.1 ± 5.73%). Each ram in both groups mated with at least 50 ewes during a breeding season.

2.2. Semen collection and washing

The animal procedures were approved by the Bahri-Dağdaş Research Center Ethical Committee, Turkey (Number: 22.12.2016/58). The rams were "trained" so that semen collection could occur utilizing an artificial vagina (AV) by allowing a ram to mount "teaser" ewes that were in estrus. When rams mounted, they were allowed to ejaculate into the AV. Before the collection of research samples, the first three collections were discarded, and then the semen was collected and processed for research use. The rams having one standard deviation greater or lesser conception rates were considered outliers regarding fertility assessments. Six rams with the greatest fertility (pregnancy rate; 98.4 ± 1.8%), and six rams having the least fertility (pregnancy rate; 76.1 ± 3.9%) (Fig. 1) were selected for proteomic profiling.

Immediately after collection of semen, a protease inhibitor (Sigma-Aldrich, Cat: P8340) (10 μl protease inhibitor/1 ml semen) was added into collection tubes. Consequently, sperm concentration was determined, and sperm cells were aliquoted (10^7 sperm/tube) and stored at −80 °C until proteomic analysis.

2.3. Proteomics

Twelve semen samples were collected from rams with the greatest and least fertility. The experimental method of proteomics was performed in the laboratory of Chemistry Group-Bioanalysis of Scientific and Technological Research Council of Turkey (TÜBİTAK), Gebze, Turkey.

2.3.1. Semen sample preparation

Sperm pellets were suspended in 50 mM ammonium bicarbonate buffer (pH 7.4). Pellets were subsequently suspended in 100 μl of lysis solution (0.25% of (w: v) (RapiGest SF, MA, USA) 5 mM dithiothreitol (Sigma-Aldrich, St. Louis, MO, USA) in 50 mM NH_4HCO_3 (Sigma-Aldrich, St. Louis, MO, USA). The samples were subsequently sonicated on ice and centrifuged at 14,000*g* at 4 °C for 5 min. Protein concentrations were subsequently determined using NanoDrop.

2.3.2. Protein digestion

Protein digestion was accomplished using a Filter-Assisted Sample Preparation digestion kit according to the manufacturer's protocol (Expedeon Inc., San Diego, CA, USA). Briefly, 100 μg of protein sample were dissolved in 200 μl of urea solution and transferred to 30 kDa cut-off colons. The sample was alkylated using 10 μl of 10X iodoacetic acid and 90 μl urea solution followed by incubation at room temperature in a darken area for 20 min. Digestion solution (40 μl containing trypsin) in 50 mM NH_4HCO_3 were added to the filters in a 50:1 protein to enzyme ratio. Samples were eluted with 40 μl of 50 mM NH_4HCO_3 and with 50 μl of sodium chloride (0.5 M) solution. The peptides were suspended in 0.1% formic acid at 150 ng/μl concentration.

2.3.3. LC/MS-MS analysis

The analysis of LC-MS/MS and identification of proteins were performed as follows: the peptides were separated using an Ultimate ™ 3000 RSLC Nano ultra-liquid chromatography system (Thermo Scientific) coupled to a Q-Exactive HF-X mass spectrometer (Thermo Fisher Scientific, Bremen, Germany) through an EASY-Spray ™ (Thermo Scientific). Tryptic peptides, reconstituted in 0.1% formic acid, were loaded onto a trap C18 PepMap100 column (300 μm i.d. × 5 mm, 5 μm particle size, 100 Å pore size) followed by elution to an analytical column (EASY-Spray PepMap™ RSLC C18, 2 μm, 100 A 75 μm × 15 cm) at a flow rate of 350 nL/min and a column temperature of 40 °C. There were 500 ng of peptides loaded in buffer A (0.1% FA, 98:2% H_2O: ACN) and separated with a buffer B (0.1% FA 98:2% ACN:H20). The separation gradient started at ranges of 3–64% ACN gradient for 179 min. The electrospray voltage applied was 2.0 kV and the capillary temperature was set to 275 °C.

The mass spectrometry data were obtained using full MS/DD-MS/MS mode. The AGC target for the full scan MS spectra was 3e6 ions in the 350–1400 *m/z* range with an IT of 100 ms and at a resolution of 60,000 at *m/z* 200. Precursor ions above the 2e5 intensity threshold were isolated with an isolation window of 1.3 *m/z*. The normalized collision energy was set at 28%. The MS/MS evaluations were performed at a resolution of 15,000 with an AGC target value of 1e5 ions.

2.4. Protein identification and quantification

The data were analyzed using MaxQuant version 1.6.11.0 to search against the reverse-decoy Uniprot *Ovis aries* database (UP000002356) with isoforms using the Andromeda search engine. A precursor mass tolerance of 0.2 Da and a fragment ion mass tolerance of 10 ppm were used. In search parameters, fixed modification of cysteine carbamidomethylation and variable modifications of oxidation and protein N-terminal acetylation were specified. The false discovery rate was set at 0.01 for peptides. Proteins were

identified with at least two peptides of a minimum length of six amino acids. Proteins were quantified using the label-free quantification (LFQ) algorithm in MaxQuant.

2.5. Bioinformatics and statistical analyses

The R package DAPAR (version 1.18.5) was used for differential analysis (Wieczorek et al., 2017). Proteins classified as 'Only identified by site', 'Potential Contaminants' and 'Reverse' were removed by filtering. Proteins that were identified in less than 12 replicates when both conditions were considered were excluded from differential abundance analysis. Partially observed missing values were imputed using the *impute.slsa* function. Significant differences in abundances of proteins for which there was a greater than 1.25-fold change (log2 FC: 0.32) were evaluated using a *limma* (limma, R package) hypothesis test with a Benjamini-Hochberg false discovery rate-adjusted *P*-values ($P < 0.05$ and FDR < 5.0%). The hierarchical clustering heat map was developed using the R platform utilizing ggplot2. There were considered to be mean differences when there was a $P < 0.05$.

2.6. Protein-protein network construction and enrichment analysis

The Protein-Protein Interaction (PPI) network was constructed using Cytoscape considering the associations which had a confidence score ≥ 0.4. The interactions were obtained from the types of evidence including experiments, databases, co-abundances, and text mining limited to "*Ovis aries*". The KEGG pathway and GO enrichments were analyzed using ClueGO V2.5.7 plug-in (Bindea et al., 2009). The ClueGO plug-in produces functionally grouped GO annotation networks for proteins. The GO categories were allotted into molecular function (MF), biological process (BP), and cellular component (CC). The *P*-value to 0.05 was set utilizing the two-sided hypergeometric tests, and Bonferroni step-down adjustment was utilized for multiple test correction. The kappa score threshold was set to 0.4.

2.7. Hub protein selection of differentially abundant proteins

The CytoScape plugin cytoHubba was exploited for the identification of important nodes by combining different topological calculations such as Maximal clique centrality (MCC), Maximum neighborhood component (MNC), Degree, Edge percolated component (EPC), and (EcCentricity) EC (Chin et al., 2014). The overlapping proteins were ranked using these five algorithms that represent the hub proteins.

3. Results

3.1. Pregnancy rates

The average pregnancy rates of all 12 rams ranged from those with the least being 76.1 ± 3.9% (pregnancy rate; $n = 6$) to those with the greatest fertility of 98.4 ± 1.8% (pregnancy rate; $n = 6$; Fig. 1).

3.2. Protein profiles of ram spermatozoa

The findings from the proteomics analysis allowed for identification of a total of 997 proteins in ram spermatozoa (Supplementary Files 1 and 2). Of the 997 proteins, 897 were identified in the sperm of GF rams while 933 were in sperm of LF rams. Among these, 840 were shared by sperm of rams in both groups, and 57 and 93 proteins were unique to rams of the GF and LF groups, respectively (Fig. 2).

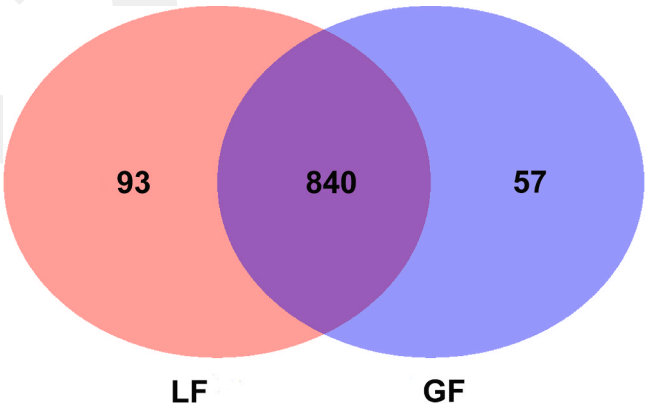

Fig. 2. Proteome profiles in sperm of GF and LF rams; Venn diagrams depict sperm proteomes of rams in GF and LF groups.

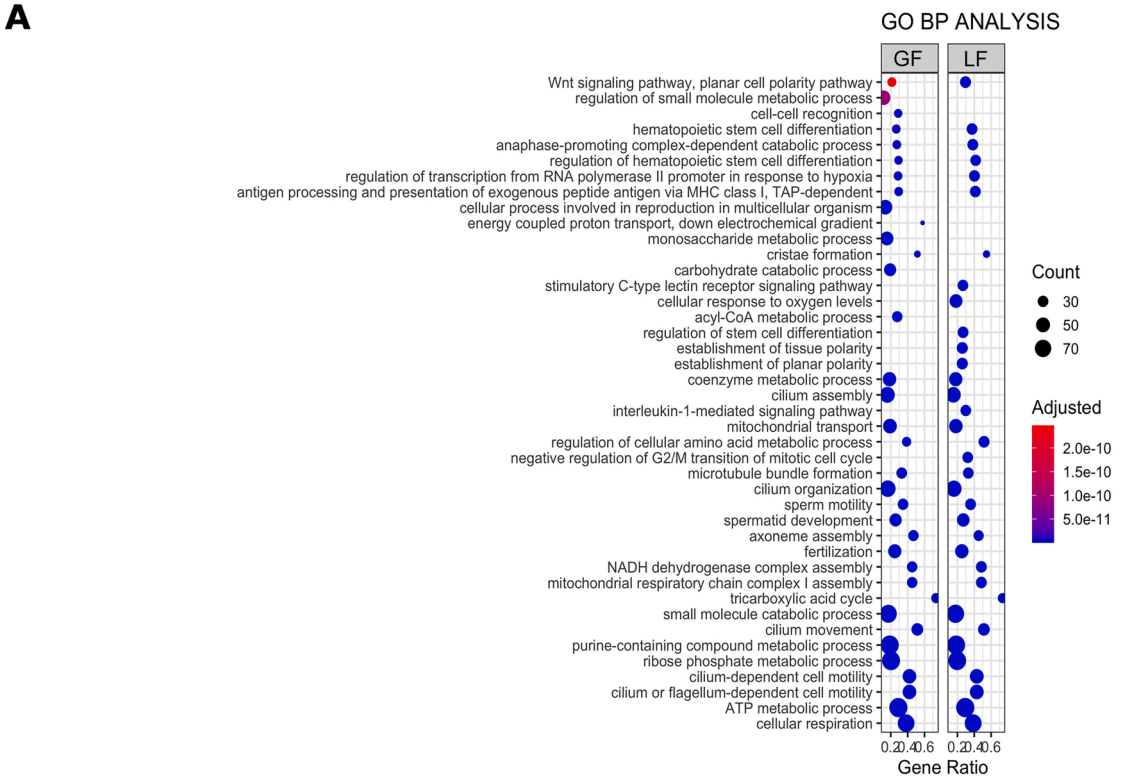

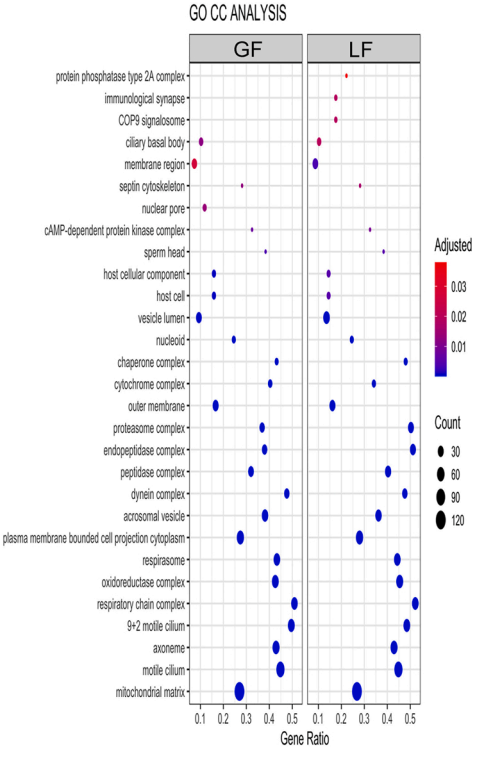

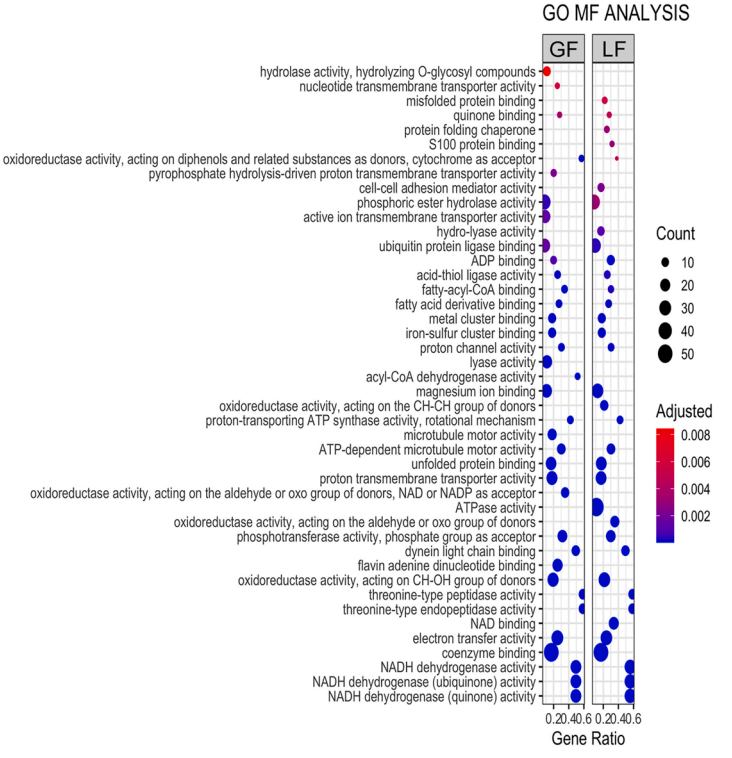

(caption on next page)

Fig. 3. Gene ontology enrichment of proteins in sperm of GF and LF rams; Gene ontology enrichment analysis of differentially abundant proteins from the rams with relatively-greater fertility (GF) and relatively-lesser fertility (LF); Bubble chart of ram proteins; a) biological process, b) cellular component, and c) molecular function; Y-axis = biological process, cellular component, and molecular function, respectively; X-axis = gene ratio, bubble size is indicative of number of abundant proteins associated with GO enrichment.

3.3. GO classification and pathway enrichment of the ram sperm protein

The GO enrichment was performed to associate relevance of the total protein abundances in sperm from GF and LF rams with the BP, MF, and CC utilizing the GO annotations (http://www.geneontology.org/GO.database.shtml; Fig. 3). Of the 897 proteins in sperm of GF rams and 993 proteins in sperm of LF rams submitted to the database there was enrichment in 575 and 584 matching GO terms in BP which were trimmed to 112 and 111 GO terms, respectively, by restriction of redundant terms based on the semantic similarity. The most frequent 42 GO terms from BP are depicted in Fig. 3a. The CC were enriched in 110 and 125 GO terms in sperm of GF and LF rams which eventually accounted for 29 significant GO terms in sperm of GF and LF rams, respectively (Fig. 3b). In MF, however, 167 GO terms were enriched in sperm of GF rams and 179 in sperm of LF rams which resulted in 55 and 61 significant GO terms, respectively. The most frequent 44 GO terms from MF are depicted in Fig. 3c. Simplified enrichments are reported in Supplementary File 4.

Overall, for GO biological process annotations, the most representative proteins were identified for cellular respiration, ATP metabolic processes, cilium or flagellum-dependent cell motility in sperm of GF and LF rams. Some of the proteins, however, were specifically classified in sperm of the GF rams, such as acyl-COA metabolic process, carbohydrate catabolic processes, and cellular processes involved in reproduction in the multicellular process while interleukin-1-mediated signaling pathway, the establishment of planar polarity, and cellular response to oxygen concentrations were annotated in sperm of LF rams (Fig. 3a). For GO cellular component, the most representative proteins were classified into the mitochondrial matrix, motile cilium, and 9 + 2 motile cilium in sperm of GF and LF rams. In sperm of GF rams, nuclear pore was the only biological process identified whereas COP9 signalosome, immunological synapse, and protein phosphatase type 2A complex annotated for sperm of LF rams (Fig. 3b). The most representative proteins for GO molecular function in sperm of GF and LF rams were NADH dehydrogenase activity, NADH dehydrogenase (ubiquinone) activity, and NADH dehydrogenase (quinone) activity (Fig. 3c).

3.4. Differentially abundant proteins in sperm of GF and LF rams

A total of 190 differentially abundant ram sperm proteins were identified when the fertility phenotype of ram spermatozoa from one group was compared with the other group (Fig. 4a). While 124 proteins were in larger abundances in the sperm of the greater as compared with lesser fertility rams, relative abundances of 66 were larger in the sperm of lesser- compared with greater-fertility rams. The list of the 15 most abundant regulated proteins in sperm of rams of the GF and LF groups are reported in Table 1. In addition, the detailed information of the differentially abundant ram sperm proteins is reported in Supplementary File 3. The heat map depicted in Fig. 4b indicates the sperm of the rams in the GF group were clearly separated from the sperm of the LF rams by the hierarchy clusters formed by differentially abundant proteins.

3.5. Protein-protein interaction (PPI) network and analysis of the functional interaction network

There was construction of a differentially abundant protein-protein interaction network including 124 proteins in sperm from rams of the GF and 66 proteins from those of the LF rams on the STRING database using Cytoscape. To evaluate the functional interaction network of the differentially abundant proteins in sperm of rams from the GF and LF groups (Fig. 5a and d, respectively), GO terms through KEGG-BioCarta pathways were utilized.

Results from the GF ram sperm indicated the 79 GO/pathway terms (Fig. 5b) that were the most significant in each group and indicated there were ten major biological networks. Of these, the three major networks were: fertilization (GO:0009566), fatty acid degradation (KEGG:00071), and monocarboxylic acid metabolic process (GO:0032787) which accounted for an 81% proportion of the total terms and the remaining proportion encompassed the acrosome vesicle (GO:0001669), protein phosphatase regulator activity (GO:0019888), hydrolase activity, acting on glycosyl bonds (GO:0016798), centriole (GO:0005814), tetrapyrrole binding (GO:0046906), carbohydrate transport (GO:0008643), and phosphoric diester hydrolase activity (GO:0008081) (Fig. 5c).

In LF ram sperm, however, there were 47 GO/pathway terms (Fig. 5e) with six major functional networks which included the nucleotide biosynthetic process (GO:0009165) with 48.9%, organelle inner membrane (GO:0019866) with 34.0% proportion, and motile cilium (GO:0031514) with 10.6% proportion, AMPK signaling (KEGG:04152) with 2.1% proportion, PPAR signaling (KEGG:03320) with 2.1% proportion, and proton transmembrane transport (GO:1902600) 2.1% proportion (Fig. 5f).

3.6. Identification of hub proteins

Following the construction of the PPI networks of differentially abundant proteins, there was identification of seven and nine hub proteins in sperm of rams from the GF and LF groups, respectively, by overlapping of the ten most abundant proteins. Proteins in the sperm of rams of the GF group were annotated as hydroxyacyl-CoA dehydrogenase trifunctional multienzyme complex subunit alpha and beta (HADHA and HADHB), enoyl-CoA delta isomerase 2 (ECI2), acyl-CoA dehydrogenase short-chain (ACADS), 3-Hydroxyisobutyryl-CoA hydrolase (HIBCH), acetyl-CoA acetyltransferase 1 (ACAT1), and acyl-CoA dehydrogenase very long chain (ACADVL) (Table 2a). Proteins in the sperm of rams of the LF group were annotated as cytochrome c oxidase subunit 5B (COX5B), ATP synthase

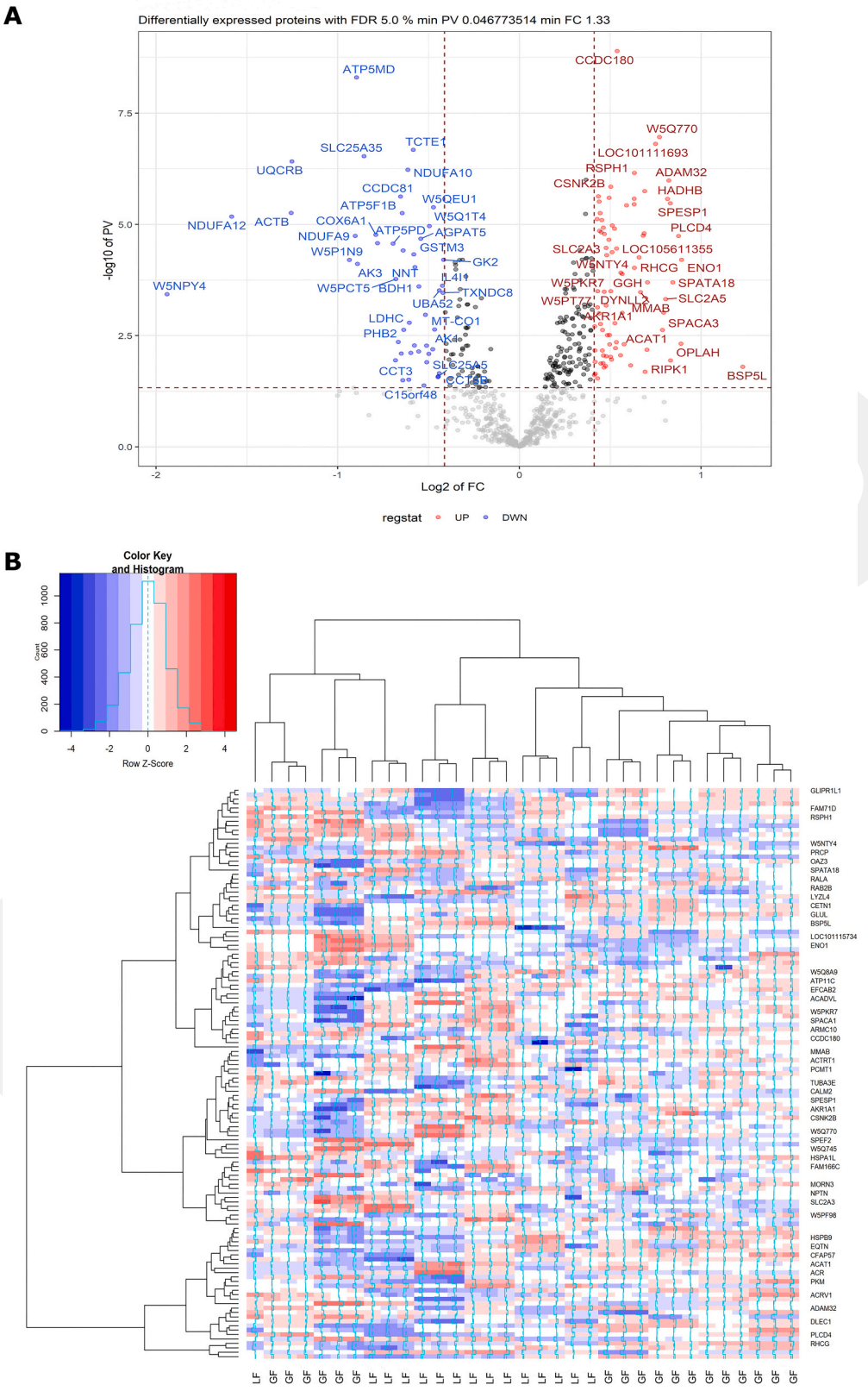
A
Differentially expressed proteins with FDR 5.0 % min PV 0.046773514 min FC 1.33
-log10 of PV
Log2 of FC
regstat UP DWN
ATP5MD
CCDC180
W5Q770
SLC25A35
TCTE1
LOC101111693
UQCRB
NDUFA10
RSPH1
ADAM32
CSNK2B
CCDC81
HADHB
ATP5F1B
W5QEU1
SPESP1
NDUFA12
ACTB
COX6A1
W5Q1T4
PLCD4
NDUFA9
ATP5PD
AGPAT5
SLC2A3
LOC105611355
W5P1N9
GSTM3
W5NTY4
RHCG
ENO1
GK2
AK3
NNT
IL4I1
W5NPY4
W5PCT5
BDH1
W5PKR7
GGH
SPATA18
TXNDC8
W5PT72
DYNLL2
SLC2A5
UBA52
MMAB
AKR1A1
LDHC
MT-CO1
SPACA3
PHB2
AK4
ACAT1
OPLAH
CCT3
SLC25A5
RIPK1
BSP5L
CCT7
C15orf48
B
Color Key and Histogram
Count
Row Z-Score
GLIPR1L1
FAM71D
RSPH1
W5NTY4
PRCP
OAZ3
SPATA18
RALA
RAB2B
LYZL4
CETN1
GLUL
BSP5L
LOC101115734
ENO1
W5Q8A9
ATP11C
EFCAB2
ACADVL
W5PKR7
SPACA1
ARMC10
CCDC180
MMAB
ACTRT1
PCMT1
TUBA3E
CALM2
SPESP1
AKR1A1
CSNK2B
W5Q770
SPEF2
W5Q745
HSPA1L
FAM166C
MORN3
NPTN
SLC2A3
W5PF98
HSPB9
EQTN
CFAP57
ACAT1
ACR
PKM
ACRV1
ADAM32
DLEC1
PLCD4
RHCG
LF GF GF GF GF GF LF LF LF LF LF LF LF LF LF LF LF GF GF GF GF GF GF GF GF GF GF GF

Fig. 4. a. Volcano plot of differentially abundant proteins in sperm of LF and GF rams; Plot depicts differentially abundant proteins; $-Log_{10}$ is plotted against the log_2 (fold change: GF: LF); Vertical lines represent ± 1.25-fold change while the horizontal line represents the significance threshold ($P < 0.05$ and FDR < 5.0%); Color coding is based on the fold change, blue; down and red; up, b. Heat map of the hierarchical clustering of differentially abundant proteins in ram sperm; Dendrogram on top depicts clustering of contrasting phenotypes of sperm from GF and LF rams, and the dendrogram on the side indicates the clustering of proteins; Colors (red; up and blue; down) represent relative protein abundances. (For interpretation of the references to color in this figure legend, the reader is referred to the web version of this article.)

subunit d and e, mitochondrial (ATP5H and ATP5I), NADH: Ubiquinone Oxidoreductase Subunit A9, A10, and A12 (NDUFA9, NDUFA10 and NDUFA12), ATP synthase, H^+ transporting, mitochondrial F1 complex, ß polypeptide (ATP5B), mitochondrial membrane ATP synthase (F(1)F(0) ATP synthase or Complex V) (ATP5A1), ubiquinol-cytochrome c reductase binding protein (UQCRB) (Table 2b).

4. Discussion

Ram sperm proteins have been characterized in several studies in which there was identification of a number of proteins that were relevant to reproductive biology (Peris-Frau et al., 2019; Pini et al., 2018). In the present study, a total of 997 ram sperm proteins were identified from rams with GF and LF phenotypes (Fig. 2). Furthermore, there were 190 differentially abundant proteins; when

Table 1
The top 15 differentially abundant proteins in sperm of rams with relatively greater (GF) or lesser (LF) fertility.

GF					LF				
Protein IDs	Gene Name	Description	Fold Change	*P*-value	Protein IDs	Gene Name	Description	Fold Change	*P*-value
W5QJB1	BSP5L	Uncharacterized protein (gene name: binder of sperm 5-like)	2.34	1.60E-02	W5PF18	LOC101102454	Uncharacterized protein	0.77	3.00E-02
W5PIG7	ENO1	Enolase 1	1.86	6.26E-05	W5QB06	LOC101103876	Uncharacterized protein	0.77	8.43E-03
W5Q173	OPLAH	5-oxoprolinase, ATP-hydrolyzing	1.85	4.82E-03	W5PWF2	ATP6V1H	V-type proton ATPase subunit H	0.78	1.46E-02
W5QED3	PLCD4	Phosphoinositide phospholipase C	1.84	1.84E-05	Q9TR28	COX7A1	Cytochrome c oxidase subunit 7A1, mitochondrial (Fragment)	0.78	8.25E-03
W5QAZ6	SPATA18	Spermatogenesis associated 18	1.79	2.01E-04	Q28554	GAPDH	Glyceraldehyde-3-phosphate dehydrogenase (Fragment)	0.78	3.93E-03
W5NTW9	RIPK1	Receptor interacting serine/threonine kinase 1	1.78	1.15E-02	W5QHI0	IMMT	MICOS complex subunit MIC60	0.78	7.20E-05
W5QB35	SPESP1	Sperm equatorial segment protein 1	1.78	3.36E-06	W5P5N9	SUN5	Sad1 and UNC84 domain containing 5	0.78	8.21E-05
W5NUY3	ADAM32	ADAM metallopeptidase domain 32	1.77	1.04E-06	W5P972	HSDL2	Hydroxysteroid dehydrogenase like 2	0.78	1.03E-04
W5QBF9	HADHB	Hydroxyacyl-CoA dehydrogenase trifunctional multienzyme complex subunit beta	1.76	2.67E-06	W5PIZ6	MLYCD	Malonyl-CoA decarboxylase	0.79	1.24E-03
Q8WMN1	SLC2A5	Solute carrier family 2, facilitated glucose transporter member 5	1.75	4.81E-04	B2MVX2	SLC25A11	SLC25A11(gene name: solute carrier family 25 member 11)	0.79	2.40E-02
W5PJE6	SPACA3	Sperm acrosome associated 3	1.73	9.63E-04	W5PD72	TSSK6	Testis specific serine kinase 6	0.79	6.82E-04
W5PN85	ACAT1	Acetyl-CoA acetyltransferase 1	1.73	2.37E-03	W5Q1L2	HSPD1	Heat shock protein family D (Hsp60) member 1	0.80	6.34E-05
W5Q770	–	Uncharacterized protein	1.71	1.09E-07	W5NRD1	ERLIN2	ER lipid raft associated 2	0.80	4.89E-04
W5PHD0	LOC101111693	Uncharacterized protein	1.68	1.55E-07	W5PYK0	EIF4A1	Eukaryotic translation initiation factor 4A1	0.80	3.89E-03
W5PNX0	SPEF2	Sperm flagellar 2	1.63	2.02E-04	W5NY50	ATP5F1A	ATP synthase subunit alpha	0.80	2.86E-04

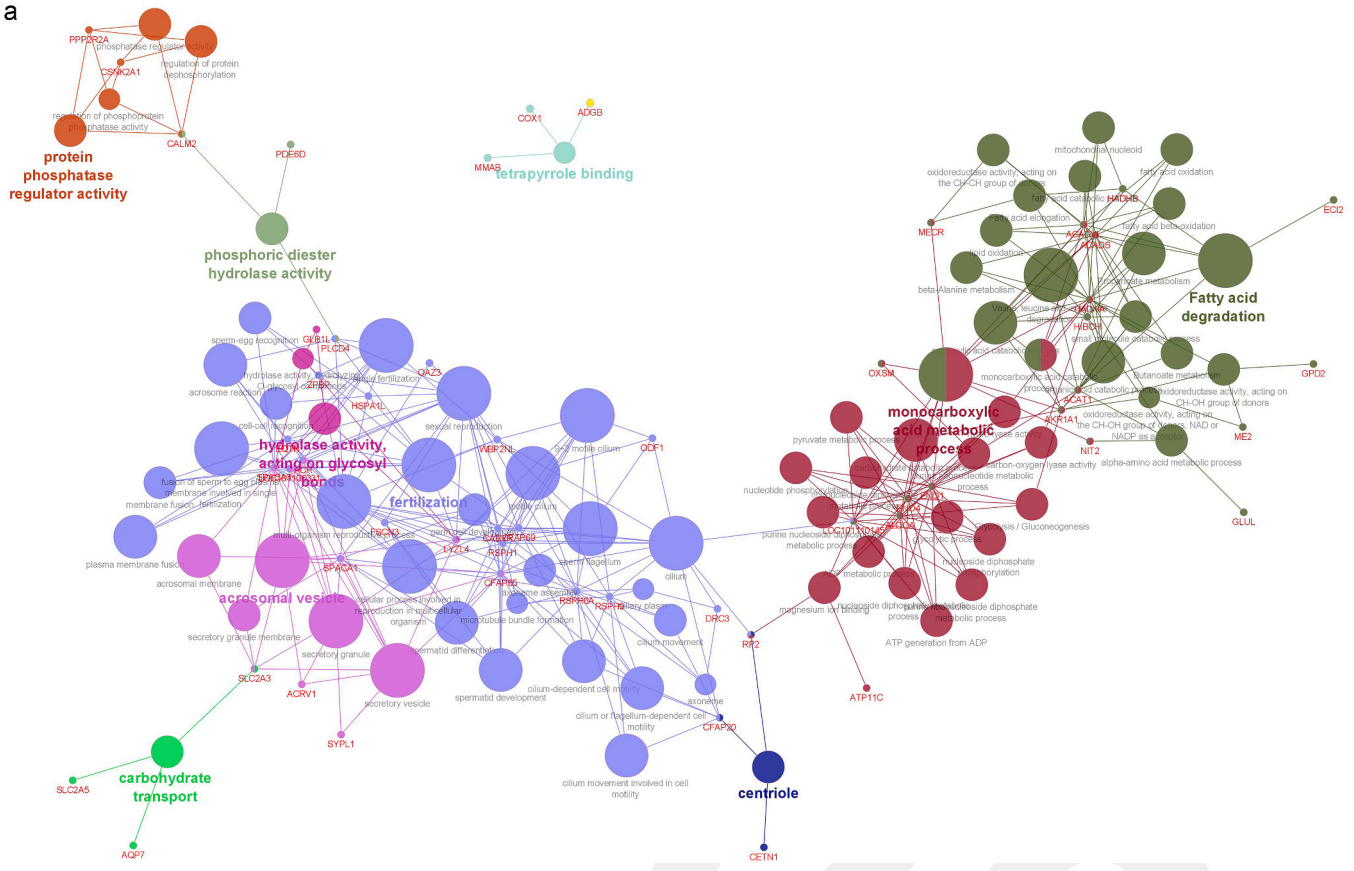

Fig. 5. a. Functional interaction of network analysis of the differentially abundant proteins in sperm of rams with relatively greater fertility (GF); GO terms are displayed as nodes, the node color depth shows different proportions of proteins; Nodes in the same cluster are designated as the same node color and node size shows the number of mapped proteins in each GO term; An edge indicates the relationship between terms; Functionally related groups partially overlap and are arbitrarily colored; b. Overview chart of functional proteins in sperm of gF rams; functional proteins indicate specific terms for differentially abundant proteins in sperm of GF rams; c. GO/pathway terms specific for sperm from GF rams; Bars depict the number of proteins associated with the terms; d. Functional interaction of network analysis of differentially abundant proteins in sperm of rams with relatively lesser fertility (LF); GO terms are depicted as nodes, node color depth depicts different abundances of proteins; Nodes in the same cluster are designated as the same node color and node size depicts number of mapped proteins in each GO term; An edge depicts the relationship between terms; Functionally related groups partially overlap and are arbitrarily colored; e. Overview chart of functional proteins in sperm of LF rams; functional proteins indicate specific terms for differentially abundant proteins in sperm of LF rams; f. GO/pathway terms specific for the proteins in sperm of LF rams; Bars depict number of proteins associated with the terms. (For interpretation of the references to color in this figure legend, the reader is referred to the web version of this article.)

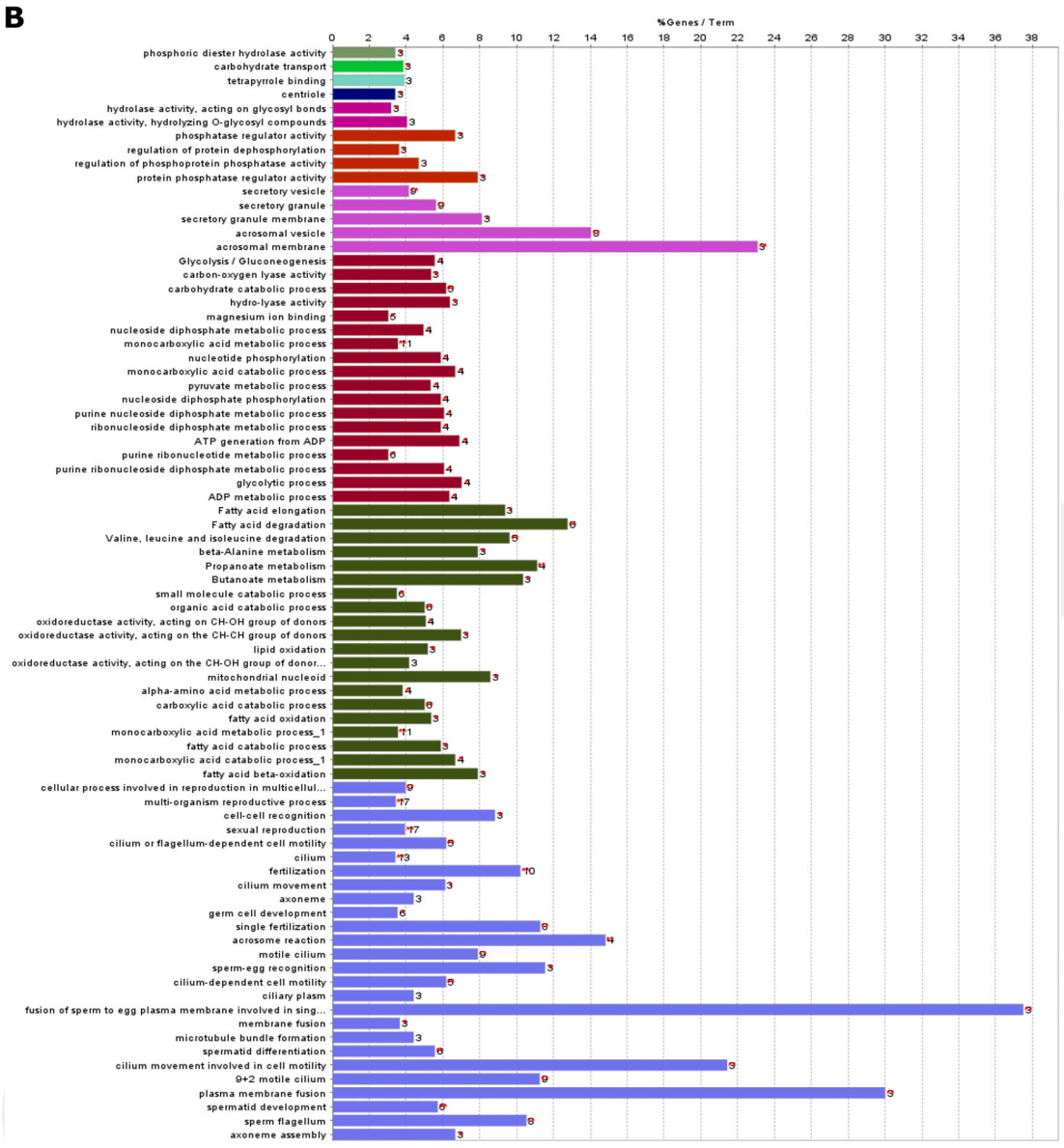

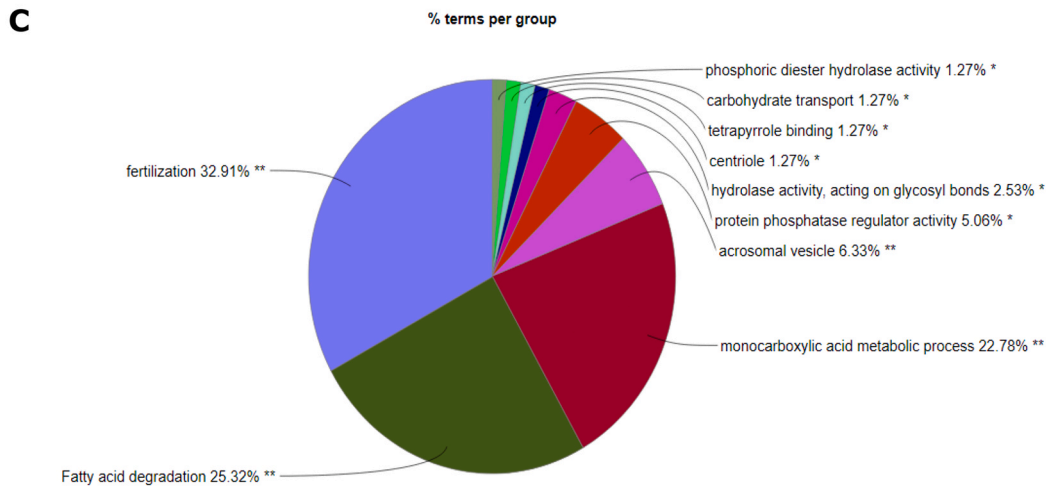

Fig. 5. (*continued*).

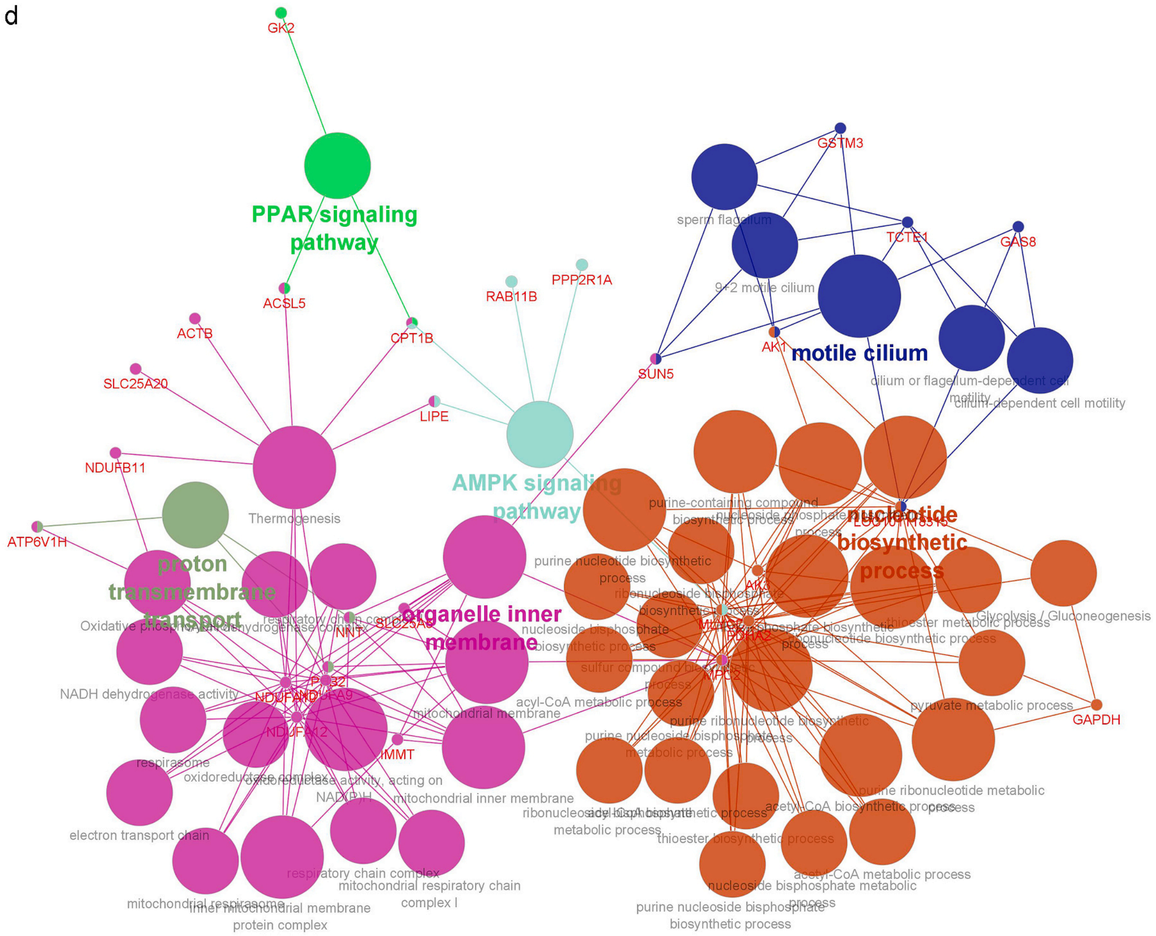

Fig. 5. (*continued*).

contrasting fertility phenotypes were compared to each other, there were greater abundances of 124 and 66 proteins in sperm of rams of the GF and LF groups, respectively (Fig. 4).

Proteins identified in GF ram sperm were mostly involved in cilia and flagellum function, thus motility (GO:0001539, GO:0005929, and GO:0060294); and there was detection of a radial spoke head protein (RSPH1, RSPH6A, and RSPH9) family which is a component of axoneme assembly (GO:0035082) (Fig. 5b). Although little is known about this family, it has been proposed to be a possible marker for signaling in flagellum (Paudel et al., 2019). In addition, of these proteins in fertilization and acrosomal vesicle network, cilia and flagella associated protein 65 and 69 (CFAP65 and CFAP69) are related to spermatogenesis and required for flagellar assembly and development (Dong et al., 2018). These proteins were enriched in fertilization (GO:0009566) and germ development (GO:0007281) as depicted in Fig. 5b, which, therefore, implies that cilia and flagellum-related proteins could be associated with ram fertility.

Among the acrosomal membrane proteins, sperm acrosome-associated 1 (SPACA1) and 3 (SPACA3) proteins were identified and these proteins modulate binding and fusion between spermatozoa and oocytes (Fujihara et al., 2012; Yamatoya et al., 2020). As such, SPACA3 has been reported to be a fertility biomarker because of functions during capacitation and the acrosome reaction (Harayama et al., 2017; Nagdas et al., 2016). In the present and previous studies, SPACA3 was the most regulated of proteins in rams with greater fertility and is involved in sexual reproduction (GO:0019953) and sperm-egg recognition (GO:0035036) (Fig. 5b). Accordingly, SPACA3 is important for fertilization and the acrosome reaction (Fig. 5a) which, therefore, may make this an important marker associated with ram fertility.

Of the 20 GO terms identified in the fatty acid degradation network (Fig. 5a), ACADS, ACADVL, ACAT1, ECI2, HADHA, HADHB, AKR1A1, and HIBCH were the most represented and, except for AKR1A1, were detected as the hub proteins (Table 2a). These proteins have important functions in metabolic pathways associated with the interaction with a network of the monocarboxylic acid metabolic process (Fig. 5a). As such, fatty acids are an essential part of structural dynamics of the sperm membrane and energy-related metabolism as well as signaling via fatty acid β-oxidation (Ferramosca et al., 2017). Propanoate and butanoate metabolism are associated with energy production and motility (Nowicka-Bauer et al., 2018). In the present study, one of the proteins enriched in propanoate metabolism (KEGG:00640) was ACADS which is involved in free fatty acid oxidation, and it modulates energy balance when

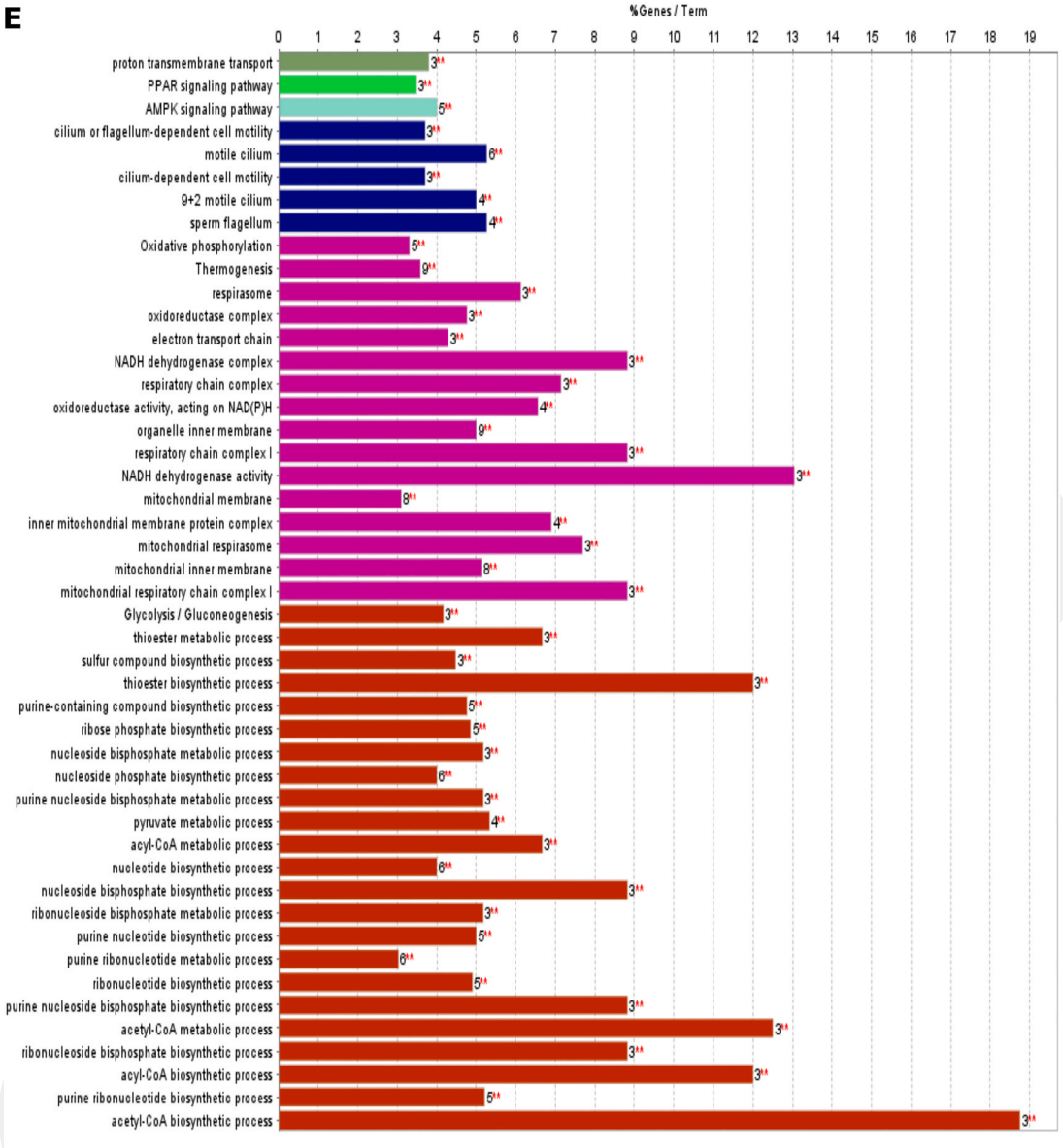

Fig. 5. (*continued*).

Table 2b
Hub proteins in sperm of rams with relatively lesser fertility (LF), ranked in cytoHubba. Overlapping hub protein symbols in top 10, MCC: Maximal cilque centrality; MNC: Maximum neighborhood component; Degree: Node degree; EPC: Edge percolated component; EC: EcCentricity.

Node Name	MCC	Node name	MNC	Node name	Degree	Node Name	EPC	Node name	EC
COX5B	14690	ATP5B	19	ATP5B	20	ATP5B	10.6	ATP5B	0.169
ATP5H	14648	COX5B	18	COX5B	18	COX5B	10.5	COX5B	0.169
NDUFA12	14576	ATP5A1	17	ATP5A1	18	ATP5A1	10.3	ATP5H	0.169
ATP5I	13800	NDUFA12	16	NDUFA12	16	NDUFA12	10.2	NDUFA12	0.169
ATP5B	12579	ATP5H	16	ATP5H	16	ATP5H	10.2	UQCRB	0.169
NDUFA10	11688	UQCRB	14	UQCRB	14	UQCRB	9.6	ATP5I	0.169
ATP5A1	11151	ATP5I	12	ATP5I	12	ATP5I	9.5	NDUFA9	0.169
UQCRB	8166	NDUFA10	12	NDUFA10	12	NDUFA10	9.3	COX1	0.169
NDUFA9	6522	NDUFA9	11	NDUFA9	11	NDUFA9	9.3	ATP5A1	0.135
COX6A1	2167	SLC25A3	9	SLC25A3	10	SLC25A3	8.5	NDUFA10	0.135

carbohydrates are not sufficiently utilized because of supplying the fat-based energy for sperm utilization (Chen et al., 2014; He et al., 2019). Propanoate-related proteins in sperm, therefore, could be the alternative resource of energy to support sustained fertility of rams with relatively greater fertility. Among the proteins identified in fatty acid beta-oxidation (GO:0006635), ACADVL modulates the inner mitochondrial membrane functions, and exogenous supply of fatty acids in boars, with primarily oleic and palmitic acids being reported to be related to greater sperm motility when there are larger abundances of ACADVL in the mid-piece of sperm (Zhu et al., 2020b). In the present study, there was also enrichment in the monocarboxylic acid metabolic network through which mammalian sperm may utilize a wide range of substrates (monocarboxylic acids) as the source of ATP production (Van Dop et al., 1977). The results confirm that this could be a primary energy source for sperm ATP production because, in a previous study, carboxylic acid and derivatives were among the major chemical classes of sperm metabolites (Menezes et al., 2019).

The two other hub proteins enriched in the fatty acid beta-oxidation pathway in sperm of rams with GF were HADHA and HADHB which catalyze three of four beta-oxidation processes (Kamijo et al., 1994). Asghari et al. (2017) estimated that these proteins have functions in ATP production which was also consistent with findings that HADHA protein deficiency leads to impaired energy generation (Das et al., 2006). While abundance of the HADHA protein has been positively associated with boar fertility, there is also the thought that it is a fertility biomarker in rams because small abundances of this protein in cryopreserved sperm is associated with lesser sperm motility as compared to fresh samples (Peris-Frau et al., 2019). In addition to HADHA, HADHB is more abundant in ejaculated ram sperm (Pini et al., 2016) which is consistent with findings in the present study that HADHB was in a larger ratio in sperm of rams in the GF group.

Enolase 1 (ENO1) was in a larger abundance in sperm of rams in the GF group, and this protein is important in the monocarboxylic acid metabolic process and is involved in the glycolysis/gluconeogenesis (KEGG:00010) pathway. The ENO1 protein has functions as a glycolytic enzyme and is one of the fertility-related proteins in bulls that could be a positive marker for fertility because abundance of this protein is positively correlated with the estrous-non-return rate (Park et al., 2019). The abundance of the ENO1 protein is also related to pregnancy rates resulting from artificial insemination (AI) with bull sperm with there being lesser pregnancy rates resulting from AI when bull sperm contain less ENO1 (Park et al., 2012; Soggiu et al., 2013). In addition to ENO1, aldolase A (ALDOA) and ENO4 have functions in fatty acid degradation, thus may be important proteins in sperm for regulation of energy generation and, therefore, ram fertility.

In the present study, there was also identification of 47 GO/pathway terms in six biological networks in rams of the LF group (Fig. 5d). Pyruvate is the most essential source of energy (Darr et al., 2016), and supplementation to extenders used for liquid preservation of sperm resulted in a greater sperm motility (Qiao et al., 2017). A functional biochemical pathway identified in sperm is pyruvate metabolism and extent of functionality is associated with bull fertility (Menezes et al., 2019). The results from this previous and current study are consistent with there being associations with the abundance of mitochondrial pyruvate carrier 2 (MPC2) protein and the activation of the pyruvate metabolic process (GO:0006090) (Fig. 5e) which occurred to a greater extent in sperm of rams in the LF group, implying that pyruvate could be important for the fertilizing capacity of ram sperm. Also, the MPC2 protein may facilitate the

Table 2a
Hub proteins in sperm of rams with relatively greater fertility (GF), ranked in cytoHubba. Overlapping hub protein symbols in top 10, MCC: Maximal cilque centrality; MNC: Maximum neighborhood component; Degree: Node degree; EPC: Edge percolated component; EC: EcCentricity.

Node name	MCC	Node name	MNC	Node name	Degree	Node name	EPC	Node name	EC
HADHA	302	HADHA	9	HADHA	10	HADHB	16.1	HADHB	0.054
HADHB	297	HADHB	9	HADHB	9	HADHA	16.0	ACAT1	0.054
ECI2	294	ECI2	8	ACAT1	9	ACAT1	16.0	HADHA	0.054
ACADS	241	ACADS	8	ECI2	8	ECI2	16.0	ECI2	0.054
HIBCH	240	HIBCH	7	ACADVL	7	ACADVL	15.7	ACADVL	0.054
ACAT1	153	ACAT1	6	HIBCH	7	ACADS	15.7	HIBCH	0.054
ACADVL	150	ACADVL	6	ACADS	6	HIBCH	15.7	ACADS	0.054
Unchr.	49	Unchr.	5	RSPH1	6	SPACA1	15.5	Unchr.	0.047
RSPH1	15	RSPH1	5	Unchr.	6	RSPH1	14.7	OXSM	0.047
RSPH9	15	RSPH9	5	RSPH9	6	Unchr.	14.6	MECR	0.044

generation of mitochondrial energy in rams of the LF group because this protein regulates pyruvate transport into the mitochondrial matrix (Lofrumento et al., 1971). Pyruvate dehydrogenase E1 alpha 2 (PDHA2), a subunit of pyruvate dehydrogenase complex, catalyzes the conversion of pyruvate to acetyl-CoA and CO_2, therefore, there is coupling of the glycolytic pathway to the tricarboxylic cycle (TCA) and as a consequence energy production. In the present study, the functional interaction network was associated with acetyl-CoA metabolic and biosynthetic processes (GO:0006084 and GO:0006085) (Fig. 5e) because acetyl-CoA is the principal substrate for the TCA, indicating this protein is important for the energetic state of sperm cells as well. Accordingly, results from the present study imply there is involvement of pyruvate metabolism and acetyl-CoA processes in energy production to maintain fertility.

Mitochondria generate ATP through oxidative phosphorylation, which occurs within the electron transport chain (ETC) consisting of five complexes, and the alterations of ETC are associated with male infertility (Ruiz-Pesini et al., 1998). The NADH dehydrogenase (Complex I) is the primary and the largest component of the mitochondrial respiratory chain which results in the transfer of electrons from NADH to the electron acceptor ubiquinone in the respiratory chain thereby constituting a proton gradient to produce ATP by ATP synthase (Saraste, 1999). Among the hub proteins, there was identification in sperm of rams of the LF group that NDUFA12, NDUFA10, and NDUFA9 were components of complex I which is involved in the organelle inner membrane biological network and are functionally associated with mitochondrial respirasome (GO:0005746) and ETC (GO:0022900) (Table 2b, Fig. 5e), thus, complex I could be the proposed site of ATP production in ram sperm. Although less is known about the functions of these proteins in the sperm cells, these proteins were only identified in a few exploratory studies as fertility-related molecules, and in the pathway of oxidative phosphorylation (Kawase et al., 2015). There is the greatest activity of complex I when there is greater rooster sperm progressive motility (Kamali Sangani et al., 2017). Consistent with results from the previous study, boar sperm, to a great extent are dependent on complex I to generate ATP and induce sperm motility (Nesci et al., 2020). In addition to complex I, a protein subunit of complex III (UQCRB) and IV (COX5B) is involved in the functions of ETC. Considering the abundance of enzymes in sperm of rams of the LF group, the regulation of these enzymes may directly affect the utilization of ATP in sperm functions.

The ATP synthase is a multi-subunit enzyme compound and initiates ATP synthesis through a proton (H+) gradient, and important functions in male fertility (Yu et al., 2019). As such, ATP5B protein abundance is larger after cryopreservation of ram spermatozoa (Pini, 2017). Also, the larger abundances of ATP5B were thought to be the reason for rapid motility of Y sperm and larger number of male offspring resulting when there are IVF procedures used (Chen et al., 2012; Hendriksen, 1999). Regarding fertility, ATP5H, ATP5B, and ATP5A1 are associated with oxidative phosphorylation that provide a diagnostic potential for bull fertility (Selvaraju et al., 2018). There is a correlation of ATP synthase protein abundance with sperm viability (Gomes et al., 2020). Results from the present study, therefore, are consistent with the previous findings that ATP synthases are hub proteins in sperm of rams with relatively lesser fertility and may modulate the utilization of ATP in sperm during fertilization processes.

5. Conclusion

The present study was to conducted to determine differentially abundant proteomes of sperm from rams with different fertility phenotypes. The differential abundance of proteins detected to be present in sperm from rams with relatively greater and lesser fertility may have functional implications as potential male fertility markers. In addition, the application of bioinformatics analyses enabled for the identification of networks that further expanded the understanding of the proteins and functions in sperm. Because of the physiological similarities among mammals, the identified proteins are also valuable in both fundamental and applied reproductive biology of other species including humans and endangered species.

Funding

This research was funded by The Scientific and Technological Research Council of Turkey (TUBITAK) with project no: (117O992) grant to Abdullah Kaya.

CRediT authorship contribution statement

Conceptualization: MH, AK, EM; Data curation: MH, AK, EM, HG, SAG; Investigation: MH, AK, EM, MÖ, MO, MB, MNB, MBA, MK, BB; Writing & editing: MH, AK, EM, MÖ, MB, SG, HG.

Declaration of competing interests

The authors declare no competing interests.

Appendix A. Supplementary material

Supplementary data associated with this article can be found in the online version at doi:10.1016/j.anireprosci.2021.106882.

References

Asghari, A., Marashi, S.A., Ansari-Pour, N., 2017. A sperm-specific proteome-scale metabolic network model identifies non-glycolytic genes for energy deficiency in asthenozoospermia. Syst. Biol. Reprod. Med. 63, 100–112. https://doi.org/10.1080/19396368.2016.1263367.

Bindea, G., Mlecnik, B., Hackl, H., Charoentong, P., Tosolini, M., Kirilovsky, A., Fridman, W.H., Pagès, F., Trajanoski, Z., Galon, J., 2009. ClueGO: a cytoscape plug-in to decipher functionally grouped gene ontology and pathway annotation networks. Bioinformatics 25, 1091–1093. https://doi.org/10.1093/bioinformatics/btp101.

Capra, E., Turri, F., Lazzari, B., Cremonesi, P., Gliozzi, T.M., Fojadelli, I., Stella, A., Pizzi, F., 2017. Small RNA sequencing of cryopreserved semen from single bull revealed altered miRNAs and piRNAs expression between high- and low-motile sperm populations. BMC Genom. 18, 14. https://doi.org/10.1186/s12864-016-3394-7.

Chen, X., Zhu, H., Wu, C., Han, W., Hao, H., Zhao, X., Du, W., Qin, T., Liu, Y., Wang, D., 2012. Identification of differentially expressed proteins between bull X and Y spermatozoa. J. Proteom. 77, 59–67. https://doi.org/10.1016/j.jprot.2012.07.004.

Chen, X., Zhu, Huabin, Hu, C., Hao, H., Zhang, J., Li, K., Zhao, X., Qin, T., Zhao, K., Zhu, Huishan, 2014. Identification of differentially expressed proteins in fresh and frozen-thawed boar spermatozoa by iTRAQ-coupled 2D LC-MS/MS. Reproduction 147, 321–330.

Chin, C.H., Chen, S.H., Wu, H.H., Ho, C.W., Ko, M.T., Lin, C.Y., 2014. cytoHubba: identifying hub objects and sub-networks from complex interactome. BMC Syst. Biol. 8, S11. https://doi.org/10.1186/1752-0509-8-S4-S11.

Darr, C.R., Varner, D.D., Teague, S., Cortopassi, G.A., Datta, S., Meyers, S.A., 2016. Lactate and pyruvate are major sources of energy for stallion sperm with dose effects on mitochondrial function, motility, and ROS production. Biol. Reprod. 95, 34. https://doi.org/10.1095/biolreprod.116.140707.

Das, A.M., Illsinger, S., Lücke, T., Hartmann, H., Ruiter, J.P.N., Steuerwald, U., Waterham, H.R., Duran, M., Wanders, R.J.A., 2006. Isolated mitochondrial long-chain ketoacyl-CoA thiolase deficiency resulting from mutations in the HADHB gene. Clin. Chem. 52, 530–534. https://doi.org/10.1373/clinchem.2005.062000.

Dogan, S., Vargovic, P., Oliveira, R., Belser, L.E., Kaya, A., Moura, A., Sutovsky, P., Parrish, J., Topper, E., Memili, E., 2015. Sperm Protamine-status correlates to the fertility of breeding bulls. Biol. Reprod. 92, 1–9. https://doi.org/10.1095/biolreprod.114.124255.

Dong, F.N., Amiri-Yekta, A., Martinez, G., Saut, A., Tek, J., Stouvenel, L., Lorès, P., Karaouzène, T., Thierry-Mieg, N., Satre, V., Brouillet, S., Daneshipour, A., Hosseini, S.H., Bonhivers, M., Gourabi, H., Dulioust, E., Arnoult, C., Touré, A., Ray, P.F., Zhao, H., Coutton, C., 2018. Absence of CFAP69 causes male infertility due to multiple morphological abnormalities of the flagella in human and mouse. Am. J. Hum. Genet. 102, 636–648. https://doi.org/10.1016/j.ajhg.2018.03.007.

Ferramosca, A., Moscatelli, N., Di Giacomo, M., Zara, V., 2017. Dietary fatty acids influence sperm quality and function. Andrology 3, 450–461. https://doi.org/10.1111/andr.12348.

Fujihara, Y., Satouh, Y., Inoue, N., Isotani, A., Ikawa, M., Okabe, M., 2012. SPACA1-deficient male mice are infertile with abnormally shaped sperm heads reminiscent of globozoospermia. Development 139, 3583–3589. https://doi.org/10.1242/dev.081778.

Gomes, F.P., Park, R., Viana, A.G., Fernandez-Costa, C., Topper, E., Kaya, A., Memili, E., Yates, J.R., Moura, A.A., 2020. Protein signatures of seminal plasma from bulls with contrasting frozen-thawed sperm viability. Sci. Rep. 10, 14661. https://doi.org/10.1038/s41598-020-71015-9.

Harayama, H., Minami, K., Kishida, K., Noda, T., 2017. Protein biomarkers for male artificial insemination subfertility in bovine spermatozoa. Reprod. Med. Biol. 16, 89–98. https://doi.org/10.1002/rmb2.12021.

He, Y., Li, H., Zhang, Y., Hu, J., Shen, Y., Feng, J., Zhao, X., 2019. Comparative analysis of mitochondrial proteome reveals the mechanism of enhanced ram sperm motility induced by carbon ion radiation after in vitro liquid storage. Dose-Response 17, 155932581882399. https://doi.org/10.1177/1559325818823998.

Hendriksen, P.J.M., 1999. Do X and Y spermatozoa differ in proteins? Theriogenology 52, 1295–1307. https://doi.org/10.1016/S0093-691X(99)00218-6.

Hitit, M., Ugur, M.R., Dinh, T.T.N., Sajeev, D., Kaya, A., Topper, E., Tan, W., Memili, E., 2020. Cellular and functional physiopathology of bull sperm with altered sperm freezability. Front. Vet. Sci. 23, 581137 https://doi.org/10.3389/fvets.2020.581137.

Kamali Sangani, A., Masoudi, A.A., Vaez Torshizi, R., 2017. Association of mitochondrial function and sperm progressivity in slow- and fast-growing roosters. Poult. Sci. 96, 211–219. https://doi.org/10.3382/ps/pew273.

Kamijo, T., Wanders, R.J.A., Saudubray, J.M., Aoyama, T., Komiyama, A., Hashimoto, T., 1994. Mitochondrial trifunctional protein deficiency. Catalytic heterogeneity of the mutant enzyme in two patients. J. Clin. Investig. 93, 1740–1747. https://doi.org/10.1172/JCI117158.

Kawase, O., Cao, S., Xuan, X., 2015. Sperm membrane proteome in wild Japanese macaque (Macaca fuscata) and Sika deer (Cervus nippon). Theriogenology 83, 95–102. https://doi.org/10.1016/j.theriogenology.2014.08.010.

Lofrumento, N.E., Papa, S., Zanotti, F., Kanduc, D., Quagliariello, E., 1971. Properties of systems of transport of anionic substrates in mitochondria. Boll. Soc. Ital. Biol. Sper. 47, 676–680.

MacLaren, A.P.C., 1988. Ram fertility in South-West Scotland. Br. Vet. J. 144, 45–54. https://doi.org/10.1016/0007-1935(88)90151-0.

Menezes, E.B., Velho, A.L.C., Santos, F., Dinh, T., Kaya, A., Topper, E., Moura, A.A., Memili, E., 2019. Uncovering sperm metabolome to discover biomarkers for bull fertility. BMC Genom. 20, 714. https://doi.org/10.1186/s12864-019-6074-6.

Menezes, E.S.B., Badial, P.R., El Debaky, H., Husna, A.U., Ugur, M.R., Kaya, A., Topper, E., Bulla, C., Grant, K.E., Bolden-Tiller, O., Moura, A.A., Memili, E., 2020. Sperm miR-15a and miR-29b are associated with bull fertility. Andrologia 52, e13412. https://doi.org/10.1111/and.13412.

Muhammad Aslam, M.K., Kumaresan, A., Yadav, S., Mohanty, T.K., Datta, T.K., 2019. Comparative proteomic analysis of high- and low-fertile buffalo bull spermatozoa for identification of fertility-associated proteins. Reprod. Domest. Anim. 54, 786–794. https://doi.org/10.1111/rda.13426.

Nagdas, S.K., Smith, L., Medina-Ortiz, I., Hernandez-Encarnacion, L., Raychoudhury, S., 2016. Identification of bovine sperm acrosomal proteins that interact with a 32-kDa acrosomal matrix protein. Mol. Cell. Biochem. 414, 153–169. https://doi.org/10.1007/s11010-016-2668-3.

Nesci, S., Spinaci, M., Galeati, G., Nerozzi, C., Pagliarani, A., Algieri, C., Tamanini, C., Bucci, D., 2020. Sperm function and mitochondrial activity: an insight on boar sperm metabolism. Theriogenology 144, 82–88. https://doi.org/10.1016/j.theriogenology.2020.01.004.

Netherton, J.K., Hetherington, L., Ogle, R.A., Velkov, T., Baker, M.A., 2018. Proteomic analysis of good-and poor-quality human sperm demonstrates that several proteins are routinely aberrantly regulated. Biol. Reprod. 99, 395–408. https://doi.org/10.1093/biolre/iox166.

Nowicka-Bauer, K., Lepczynski, A., Ozgo, M., Kamieniczna, M., Fraczek, M., Stanski, L., Olszewska, M., Malcher, A., Skrzypczak, W., Kurpisz, M.K., 2018. Sperm mitochondrial dysfunction and oxidative stress as possible reasons for isolated asthenozoospermia. J. Physiol. Pharmacol. 69, 403–414. https://doi.org/10.26402/jpp.2018.3.05.

Özbek, M., Hitit, M., Kaya, A., Jousan, F.D., Memili, E., 2021. Sperm functional genome associated with bull fertility. Front. Vet. Sci. 0, 571. https://doi.org/10.3389/FVETS.2021.610888.

Panner Selvam, M.K., Agarwal, A., Pushparaj, P.N., 2019. A quantitative global proteomics approach to understanding the functional pathways dysregulated in the spermatozoa of asthenozoospermic testicular cancer patients. Andrology 7, 454–462. https://doi.org/10.1111/ANDR.12620.

Pardos, L., Rubio, M.T.M., Fantova, E., 2008. The diversity of sheep production systems in Aragón (Spain): characterisation and typification of meat sheep farms. Span. J. Agric. Res. 6, 497–507.

Park, Y.J., Kwon, W.S., Oh, S.A., Pang, M.G., 2012. Fertility-related proteomic profiling bull spermatozoa separated by percoll. J. Proteome Res. 11, 4162–4168. https://doi.org/10.1021/pr300248s.

Park, Y.-J., Pang, W.-K., Ryu, D.-Y., Song, W.-H., Rahman, M.-S., Pang, M.-G., 2019. Optimized combination of multiple biomarkers to improve diagnostic accuracy in male fertility. Theriogenology 139, 106–112. https://doi.org/10.1016/J.THERIOGENOLOGY.2019.07.029.

Paudel, B., Gervasi, M.G., Porambo, J., Caraballo, D.A., Tourzani, D.A., Mager, J., Platt, M.D., Salicioni, A.M., Visconti, P.E., 2019. Sperm capacitation is associated with phosphorylation of the testis-specific radial spoke protein Rsph6a. Biol. Reprod. 100, 440–454. https://doi.org/10.1093/biolre/ioy202.

Peris-Frau, P., Martín-Maestro, A., Iniesta-Cuerda, M., Sánchez-Ajofrín, I., Mateos-Hernández, L., Garde, J.J., Villar, M., Soler, A.J., 2019. Freezing-thawing procedures remodel the proteome of ram sperm before and after in vitro capacitation. Int. J. Mol. Sci. 20, 4596. https://doi.org/10.3390/ijms20184596.

Pini, T., Leahy, T., Soleilhavoup, C., Tsikis, G., Labas, V., Combes-Soia, L., Harichaux, G., Rickard, J.P., Druart, X., De Graaf, S.P., 2016. Proteomic investigation of ram spermatozoa and the proteins conferred by seminal plasma. J. Proteome Res. 15, 3700–3711. https://doi.org/10.1021/acs.jproteome.6b00530.

Pini, T., Rickard, J.P., Leahy, T., Crossett, B., Druart, X., de Graaf, S.P., 2018. Cryopreservation and egg yolk medium alter the proteome of ram spermatozoa. J. Proteom. 181, 73–82. https://doi.org/10.1016/j.jprot.2018.04.001.

Pini, T., 2017. Studies on the Modification of Ram Spermatozoa by Ejaculation and Cryopreservation and the Effects of Binder of Sperm Proteins, University of Sydney.

Pixton, K.L., Deeks, E.D., Flesch, F.M., Moseley, F.L.C., Björndahl, L., Ashton, P.R., Barratt, C.L.R., Brewis, I.A., 2004. Sperm proteome mapping of a patient who experiencd failed fertilization at IVF reveals altered expression of at least 20 proteins compared with fertile donors: case report. Hum. Reprod. 19, 1438–1447. https://doi.org/10.1093/humrep/deh224.

Qiao, S., Wu, W., Chen, M., Tang, Q., Xia, Y., Jia, W., Wang, X., 2017. Seminal plasma metabolomics approach for the diagnosis of unexplained male infertility. PLoS One 12, e0181115. https://doi.org/10.1371/journal.pone.0181115.

Rathke, C., Baarends, W.M., Awe, S., Renkawitz-Pohl, R., 2014. Chromatin dynamics during spermiogenesis. Biochim. Biophys. Acta Gene Regul. Mech. 1839, 155–168. https://doi.org/10.1016/j.bbagrm.2013.08.004.

Ruiz-Pesini, E., Diez, C., Lapena, A.C., Perez-Martos, A., Montoya, J., Alvarez, E., Arenas, J., Lopez-Perez, M.J., 1998. Correlation of sperm motility with mitochondrial enzymatic activities. Clin. Chem. 44, 1616–1620. https://doi.org/10.1093/clinchem/44.8.1616.

Saraste, M., 1999. Oxidative phosphorylation at the fin de siecle. Science 283, 1488–1493. https://doi.org/10.1126/science.283.5407.1488 (80-.).

Selvaraju, S., Parthipan, S., Somashekar, L., Binsila, B.K., Kolte, A.P., Arangasamy, A., Ravindra, J.P., Krawetz, S.A., 2018. Current status of sperm functional genomics and its diagnostic potential of fertility in bovine (Bos taurus). Syst. Biol. Reprod. Med. 64, 484–501. https://doi.org/10.1080/19396368.2018.1444816.

Soggiu, A., Piras, C., Hussein, H.A., De Canio, M., Gaviraghi, A., Galli, A., Urbani, A., Bonizzi, L., Roncada, P., 2013. Unravelling the bull fertility proteome. Mol. Biosyst. 9, 1188–1195. https://doi.org/10.1039/c3mb25494a.

Van Dop, C., Hutson, S.M., Lardy, H.A., 1977. Pyruvate metabolism in bovine epididymal spermatozoa. J. Biol. Chem. 252, 1303–1308. https://doi.org/10.1016/S0021-9258(17)40655-7.

Wieczorek, S., Combes, F., Lazar, C., Gianetto, Q.G., Gatto, L., Dorffer, A., Hesse, A.M., Couté, Y., Ferro, M., Bruley, C., Burger, T., 2017. DAPAR & ProStaR: software to perform statistical analyses in quantitative discovery proteomics. Bioinformatics 33, 135–136. https://doi.org/10.1093/bioinformatics/btw580.

Yamatoya, K., Kousaka, M., Ito, C., Nakata, K., Hatano, M., Araki, Y., Toshimori, K., 2020. Cleavage of SPACA1 regulates assembly of sperm-egg membrane fusion machinery in mature spermatozoa. Biol. Reprod. 102, 750–757. https://doi.org/10.1093/biolre/ioz223.

Yu, J., Chen, B., Zheng, B., Qiao, C., Chen, X., Yan, Y., Luan, X., Xie, B., Liu, J., Shen, C., He, Z., Hu, X., Liu, M., Li, H., Shao, Q., Fang, J., 2019. ATP synthase is required for male fertility and germ cell maturation in Drosophila testes. Mol. Med. Rep. 19, 1561–1570. https://doi.org/10.3892/mmr.2019.9834.

Zhu, W., Zhang, Y., Ren, C. huan, Cheng, X., Chen, J. hong, Ge, Z. yong, Sun, Z. peng, Zhuo, X., Sun, F. fei, Chen, Y. le, Jia, X. jiao, Zhang, Z., 2020a. Identification of proteomic markers for ram spermatozoa motility using a tandem mass tag (TMT) approach. J. Proteom. 210, 103438 https://doi.org/10.1016/j.jprot.2019.103438.

Zhu, Z., Li, R., Feng, C., Liu, R., Zheng, Y., Hoque, S.A.M., Wu, D., Lu, H., Zhang, T., Zeng, W., 2020b. Exogenous oleic acid and palmitic acid improve boar sperm motility via enhancing mitochondrial B-oxidation for ATP generation. Anim. Open Access J. MDPI 10, 591. https://doi.org/10.3390/ANI10040591.